

Inside-out Galaxy Formation

Jeremy V. Kepner

Princeton University Observatory

Peyton Hall, Ivy Lane, Princeton, NJ 08544-1001

jvkepner@astro.princeton.edu

Current address: MIT Lincoln Laboratory, Lexington, MA

ABSTRACT

Current theories of galaxy formation have tended to focus on hierarchical structure formation, which is the most likely scenario for cosmological models with lots of power at small scales (e.g. standard cold dark matter). Models with little small scale power lead to scenarios closer to spherical collapse. Recently favored power spectra (e.g. CDM+ Λ) lie somewhere in between suggesting that both types of processes are important and may vary over time due to gaseous reheating. From this viewpoint this paper explores a very simple inside out scenario for galaxy formation. This scenario is a natural result of synthesizing earlier work on DM halos, spherical collapse, and gas redistribution via angular momentum. Although, this model is highly simplified and is not designed to accurately describe the detailed formation of any individual galaxy, it does (by design) predict the overall features of galaxies. In addition, old bulges and young disks are an almost unavoidable result of these very simple models. This scenario may provide a useful framework for both observers and theoreticians to think about galaxy formation.

1. Introduction

Galaxy formation theories can be caricatured by two models: hierarchical clustering and spherical collapse; with reality most likely lying somewhere in between. The degree of hierarchical clustering is strongly dependent upon the amount of power on small scales. Cosmological models with lots of small scale power (e.g., standard CDM) will be more hierarchical, while many of the cosmological models currently under consideration have power spectra with less small scale power (e.g., mixed dark matter, tilted CDM+ Λ) (Borgani et al 1997) and will be less hierarchical.

The thermal history of the gas can also play an important role. At early epochs the gas temperature will be low, which allows small lumps to form and be accreted hierarchically. At later epochs, the IGM heats up to $\sim 10^4$ °K due to the first generation of stars and Quasar emission. Gas at this temperature will be driven out of halos with circular velocities less than 30 km s^{-1} (Kepner, Babul & Spergel 1997). Accretion of these small lumps at $z \sim 3$ may not take place hierarchically but will tend towards spherical infall as the puffed up lumps of gas encounter gas in

the halo that has been heated by shocks and radiation from a variety of sources: stars, supernova, and possibly a supermassive black hole. In reality, the gas in galaxy formation is most likely in multiple phases (like the present day galaxy).

Exploring both hierarchical and spherical collapse aspects of galaxy formation is best accomplished with a variety of techniques. N-body simulations are best for exploring hierarchical structure formation. Detailed simulations of the formation of individual galaxies can now be performed with an ever increasing list of physical processes. Some of the important results of simulations are the approximate correctness of Press-Schechter theory for describing merging histories (Lacey & Cole 1994), that dark matter (DM) halos have a similar form over a wide range of scales (Navarro, Frenk & White 1996), and the nature of the Ly α forest (Miralda-Escude et al 1996, Ma et al 1997, Zhang et al 1997). In addition, simulations that include gas dynamics show development of disks as a result of tidal torques (Navarro & Steinmetz 1997, Steinmetz & Ewald 1995).

Analytic methods lend themselves to the understanding of spherical collapse. The original analytic work on spherical collapse (Gunn & Gott 1972, Fillmore & Goldreich 1984, Bertschinger 1985) laid the groundwork for understanding virialization, self-similar collapse, the establishment of near isothermal dark matter halos, and secondary infall. More recent analytic work has been particularly useful in providing intuition on the formation of disk galaxies (Dalcanton, Spergel & Summers 1997, Mo, Mao & White 1997), an area that is particularly challenging for N-body simulations due to the large dynamic range requirements. These recent analytic papers, built upon the earlier work of Mestel 1963, Fall & Efstatihou 1980, and Gunn 1982, indicates that allowing gas with typical angular momentum distributions to settle into typical DM halos produces disk galaxies that reproduce a wide variety of observations from faint surface brightness objects to damped Ly α systems. The fundamental assumptions of Dalcanton, Spergel & Summers 1997 and Mo, Mao & White 1997, which will also be adopted in this paper, are that (1) there is little angular momentum transport, and (2) the angular momentum eventually halts the collapse of the gas, resulting in a roughly flat rotation curve.

Spherically symmetric analytic models have a limited ability to address highly non-linear phenomena such as hydrodynamic shocks. Recent spherical numerical simulations of infall into galaxies indicate that gas can undergo a shock before settling into the DM potential (Thoul & Weinberg 1995). Such shocks are potentially an important process for slowing down and heating infalling gas during galaxy formation.

The goal of this paper is to add to the analytical understanding of galaxy formation by connecting the earlier spherical collapse models with the more recent work on redistribution by angular momentum and infall shocks. The approach is quite simple. Given a known approximate initial state—some kind of primordial “bump” (Bardeen et al 1986), and a known approximate final state of the DM halo and the gaseous disk, completing the picture requires determining the time, mass and length scales for the transformation of the DM and the gas from the initial state to

the final state. The collapse and virialization of spherically symmetric DM halos gives an estimate of the scales involved in creating a DM halo. The scales for gaseous collapse can likewise be set by the evolution of an outwardly moving shock (Thoul & Weinberg 1995).

Synthesizing these two components results in a single physically motivated scenario which, by construction, reproduces many of the observable quantities of the final states of galaxies, but also makes specific predictions about gas evolution during galaxy formation. Such a scenario can be a useful perspective for both observers and theoreticians by clarifying the important quantities to be measured and the additional physical processes that need to be included to explain various phenomena.

In §2 a sketch of the inside-out galaxy formation scenario is presented along with an overview of the underlying physics. In §3 the physical model is presented in detail. §4 discusses the results of these calculations. §5 gives conclusions and plans for further work.

2. Inside-out Galaxy Formation

Any exploration of galaxy formation begins with a list of ingredients. The two main components are dark matter and gas. In this paper it is assumed that the dark matter is cold and collisionless. The gas can behave in a variety of ways depending upon its thermal history. If the gas is dense it can radiate away heat acquired in shocks and will tend to behave in a relatively cold manner. If the gas is diffuse it may be heated by external radiation or shocks. Recent simulations of infalling gas with radiative cooling indicates that such shocks occur in a variety of galactic potentials (Thoul & Weinberg 1995). Furthermore, these simulations suggest that the initial radius at which a mass shell is shocked is similar in both the adiabatic and non-adiabatic cases. Thus the simplest approach is to use a adiabatic numerical approach to calculate the initial shock radius and then use analytic non-adiabatic methods to estimate the post-shock behavior. In reality, the gas in galaxy formation is most likely in multiple phases (like the present day galaxy). Of course, the limits of the adiabatic approximation for computing the shock radius must be kept in mind in interpreting any subsequent results.

The inside-out scenario that results from combining spherical collapse and angular momentum redistribution proceeds as follows. Initially the gas and dark matter are coupled and expand with the Hubble flow. The innermost shells turn around first. The dark matter virializes, and the gas is shock heated to the virial temperature. The cooling time for these inner shells is very short and some of the gas may quickly condense into cold lumps and form bulge stars. Later, the outermost shells turn around and their gas is shock heated. However, for these outer shells, the higher virial temperatures and lower gas densities result in longer cooling times; so that as the gas cools and falls to its corresponding angular momentum radius it is shocked again and forms stars. Higher angular momentum material ends up outside the bulge and forms the disk. Lower angular momentum material falls into the bulge, which continues to grow slowly, but may be halted by

energy input from supernova and/or a massive black hole that can initiate a wind that blows out the gas.

The two components of the above scenario are DM and gas. In the next two sub-sections the specific evolution of each component is elaborated. In addition, some of the concepts that form the basis of the physical model will also be introduced.

2.1. DM Evolution

Typically, a spherical dark matter halo is quantified by a characteristic mass and radius ($M_{\text{halo}}, r_{\text{halo}}$), which can be translated into a circular velocity and virialization redshift ($V_{\text{circ}}, z_{\text{virial}}$) by assuming a value for the overdensity at z_{virial} (e.g., $\delta_{\text{virial}} \sim 179$). Simple estimates of the number of halos of a given mass at each redshift can be made via the Press-Schechter formalism. These estimates provide useful insights into the size distribution of DM halos and are in approximate agreement with galaxy catalogs and N-body simulations.

As primordial DM halos initially expand and contract they are torqued by neighboring density peaks leaving some galaxies with significant amounts of angular momentum. The amount of angular momentum is characterized by the spin parameter λ_{spin} . Galaxies with larger values of λ_{spin} form disks. Thus three parameters would seem to describe the gross characteristics of galaxies ($M_{\text{halo}}, r_{\text{halo}}, \lambda_{\text{spin}}$) or equivalently ($V_{\text{circ}}, z_{\text{virial}}, \lambda_{\text{spin}}$).

For an idealized spherically symmetric DM halo, the evolution is qualitatively quite simple. Each mass shell in a primordial “bump” proceeds through Hubble expansion, turn around, virialization and relaxation into a final quasi-stationary DM profile. This process is characterized by the collapse time t_{collapse} and the maximum radius r_{max} of each bound DM shell.

The initial bump can be estimated via various theoretical arguments and the result can usually be fit by an approximately Gaussian profile. The final DM profiles have been extensively studied both observationally and via N-body simulations and a variety of universal profiles have been proposed. These differ in detail but produce similar rotation curves, $V_{\text{circ}}(r)$, over the observationally accessible radii (see Figure 1). The process of virialization has also been extensively studied in simulations. There is no simple way to characterize this process. Fortunately, for spherical collapse this process seems to take place fairly quickly and in a manner which tends to erase the details of the initial distribution (Hoffman 1988).

An asymptotically correct model of the DM evolution can be constructed by marrying the initial expansion and turn around of a pre-determined initial profile with a pre-determined final profile by simply stopping each infalling mass shell at the radius set by the final profile. Such a model—while completely sidestepping the important role of virialization and hierarchical structure formation—provides a simple framework for describing the DM potential and its effect on the gas.

2.2. Gaseous Evolution

For the most part, each gas shell of the galaxy evolves passively under the gravitational influence of the dark matter until it collapses. In the case of adiabatic gas, the inner shells will be compressed until there is sufficient pressure to stop the infall and create a shock. This process is characterized by the shock time t_{shock} and shock radius r_{shock} of each mass shell which define the pertinent time and length scales of the gas in the halo. Inside the shock, the gas will be approximately in isothermal hydrostatic equilibrium with a temperature given by the DM potential at r_{shock} . Outside the shock, the gas will be cooler and significantly less dense. In a real multi-phase gas, r_{shock} can be thought of as an approximate upper limit for the radius at which cooler clumps of gas begin to feel the effects of the external environment. The “true” radius will be somewhat smaller to account for the fraction of gas that has condensed into cold lumps. Some simulations indicate that early on this can be a large fraction of the gas (Navarro & Steinmetz 1997). Later on the ratio of cold gas to shocked gas can be as low as 20% (Thoul & Weinberg 1995), suggesting that the adiabatic value of r_{shock} becomes more accurate at later times.

The main effects of the shock are twofold. First, the dissipation of a significant amount of inward velocity results in the slow spiraling of any cool clumps towards their corresponding angular momentum radii. Second, a large increase in density leads to a dramatic drop in the cooling time $t_{\text{cool}} \propto \rho_{\text{gas}}^{-1}$. If the cooling time is short compared to the dynamical time $t_{\text{dyn}} = \pi r V_{\text{circ}}^{-1}$, then even the clumps in the hot gas will condense and may undergo rapid star formation, otherwise they will spiral inwards until they hit the disk. The initial gas mass and radius of this region, which may correspond to an initial bulge, can be computed by setting $t_{\text{dyn}} = t_{\text{cool}}$. Subsequent mass shells will split their material between the bulge region and the disk depending upon the distribution of specific angular momentum within each mass shell. The bulge will continue to grow slowly. However, this process can be halted if there is sufficient energy input from supernovae and/or a massive black hole to drive a wind. The disk will continue to grow outward as long as there is infalling material to supply it.

Asymptotically redistributing the gas according to its angular momentum produces disks in agreement with a wide variety of observations (Dalcanton, Spergel & Summers 1997, Mo, Mao & White 1997). Thus, as with the DM halo, there is a fairly good picture of the early and late stages of the gas. The evolving adiabatic shock is a means for setting the time, length and mass scales of the evolution of the gas between these states.

3. Physical Model

The previous section gave a broad overview of an inside-out scenario for galaxy formation and hinted at the underlying physical model used to motivate it. In this section the details are presented. First, the final DM halo is described. Second, the evolution of the DM halo from a primordial bump is discussed. Third, the evolution of the shock radius of the gas is presented.

Fourth, the initial formation of the bulge is computed. Fifth, the infall of material onto the bulge and the disk is derived. Sixth, the processes that may lead to a wind are discussed.

3.1. Final DM halo

Let the final dark matter halo be specified by two parameters: the halo radius and halo mass, which can be translated into the circular velocity V_{circ} and the virialization redshift z_{virial} if it is assumed that the overdensity at virialization is $\delta_{\text{virial}} \sim 179$ (Gunn & Gott 1972)

$$V_{\text{circ}}^2(r_{\text{halo}}) = \frac{GM_{\text{halo}}}{r_{\text{halo}}} , \quad \frac{4\pi}{3}r_{\text{halo}}^3\delta_{\text{virial}}\rho_{\text{crit}}(z_{\text{virial}}) = M_{\text{halo}}, \quad (1)$$

where the mean density is given by the usual expressions for a $\Omega = 1$ CDM cosmological model: $\rho_{\text{crit}}(z) = (1+z)^3\rho_{\text{crit}}^0$, $6\pi G\rho_{\text{crit}}t_{\text{universe}}^2 = 1$, $t_{\text{universe}}^0 = 2/3H_0$. The distribution within the DM halo can be any reasonable profile (e.g. Hernquist 1990, Burkert 1995, Navarro, Frenk & White 1996, see Figure 1), which satisfies the above equations at r_{halo} . The simplest choice is an isothermal sphere for which:

$$M_{\text{DM}}(r) = \frac{M_{\text{halo}}}{r_{\text{halo}}}r , \quad V_{\text{circ}}(r) = V_{\text{circ}}(r_{\text{halo}}) , \quad \rho_{\text{DM}}(r) = \frac{M_{\text{halo}}}{r_{\text{halo}}}\frac{1}{4\pi r^2} \quad (2)$$

3.2. Primordial bump

The simplest description of the state of a DM halo at some early epoch (corresponding to redshift z_{init}) is a spherical “bump” in the density field $\rho_{\text{DM}}(r, z_{\text{init}})$. A typical initial density profile might be (see Figure 2):

$$\rho_{\text{DM}}(r, z_{\text{init}}) = \rho_{\text{crit}}(z_{\text{init}}) + \rho_0 e^{-r^2/r_{\text{halo}}^2(z_{\text{init}})} \quad (3)$$

The dynamics of each mass shell in the halo are governed by the interior overdensity:

$$\delta_{\text{DM}}(r) + 1 = \frac{M_{\text{DM}}(r)}{\frac{4\pi}{3}r^3\rho_{\text{crit}}(z_{\text{init}})} \quad (4)$$

where $M_{\text{DM}}(r) = \int_0^r 4\pi r'^2 \rho_{\text{DM}}(r') dr'$. δ_{DM} determines the Hubble flow for each point at z_{init} via the linear theory estimate (Thoul & Weinberg 1995)

$$v_{\text{DM}}(r, z_{\text{init}}) = rH(z_{\text{init}})[1 - \frac{1}{3}\delta_{\text{DM}}(r)]. \quad (5)$$

The above estimate will be accurate while $\delta_{\text{DM}} \ll 1$.

Having specified the initial position, velocity and time of each mass shell the subsequent evolution is governed by

$$2\pi \frac{t}{t_{\text{collapse}}} = \theta - \sin \theta , \quad \frac{2r}{r_{\text{max}}} = 1 - \cos \theta , \quad v_{\text{DM}} = \frac{\pi \sin \theta}{1 - \cos \theta} \frac{r_{\text{max}}}{t_{\text{collapse}}}, \quad (6)$$

where

$$\frac{1}{r_{\max}(r)} = \frac{1}{r} - \frac{v(r)}{2GM_{\text{DM}}(r)}, \quad t_{\text{collapse}}(r) = 2\pi \sqrt{\frac{r_{\max}^3}{8GM(r)}} \quad (7)$$

The above description of the trajectories holds as long as there are no shell crossings. Unfortunately, there is no elegant procedure to ensure collapsing shells virialize into a desired quasi-stationary DM halo. The simplest method, which is adopted here, is to stop each mass shell when it reaches a pre-determined final radius. It remains to be seen whether or not this approach provides a sufficiently accurate picture of the DM potential from the point of view of the gas. Figure 3 shows the trajectories of various mass shells when this method is employed with an isothermal profile.

3.3. Shock Radius

Detailed spherical collapse calculations (Thoul & Weinberg 1995; Thoul & Weinberg 1996) indicate that gas falling into a variety of galaxy potentials undergoes a shock. These simulations were conducted for both adiabatic and non-adiabatic gas (using standard cooling functions) in a fully dynamical DM potential. One important observation of these simulations is that the initial shock radius in both adiabatic and non-adiabatic gas is similar. However, after the initial shock the gas cannot be treated adiabatically. While a non-adiabatic model in a fully dynamic DM potential provides a richer description of galaxy formation it is more difficult to develop a simple relations for the shock radius from such simulations. This would suggest that the simplest means for obtaining an expression of the initial shock radius is to examine adiabatic gas falling into a deterministically evolving DM potential. After obtaining this relation, a non-adiabatic analytic approach is adopted in the next sub-section to look at the post-shock behaviour of the gas.

The adiabatic evolution of the gas within the above evolving DM potential is governed by the Lagrangian equations:

$$\begin{aligned} \frac{d}{dr}M_{\text{gas}} &= 4\pi r^2 \rho_{\text{gas}}, \\ \frac{d}{dt}v_{\text{gas}} &= -4\pi r^2 \frac{dP_{\text{gas}}}{dM_{\text{gas}}} - \frac{GM_{\text{DM}}(r)}{r^2}, \\ \frac{d}{dt}u_{\text{gas}} &= \frac{P_{\text{gas}}}{\rho_{\text{gas}}^2} \frac{d}{dt}\rho_{\text{gas}}, \\ P_{\text{gas}} &= (\gamma - 1)\rho_{\text{gas}}u_{\text{gas}}, \end{aligned} \quad (8)$$

where the self-gravity of the gas has been ignored because it becomes important only in the inner regions of the bulge and the disk, well inside the shock. For the relevant initial conditions ($\rho_{\text{gas}}(r) = \Omega_{\text{baryon}}\rho_{\text{DM}}(r)$, $v_{\text{gas}}(r) = v_{\text{DM}}(r)$), the global behavior of the solutions to the above equations are quite similar: the gas expands and contracts with the DM until the pressure gradient stops the infall and causes a shock to form. Inside the shock the gas is hot and dense, while outside

the shock it is cool and less dense. Thus, the evolution of the shock front describes, to first order, the overall behavior of the gas. The shock occurs when the infall speed of a shell approximately equals the thermal speed of the gas interior to it. If the gas is assumed to follow the DM until this point, and that inside the shock the gas is at a temperature corresponding to the circular velocity of the DM halo, then the shock will occur when:

$$V_{\text{circ}}(r_{\text{shock}}) = v_{\text{gas}}(M_{\text{shock}}) \approx v_{\text{DM}}(M_{\text{shock}}/\Omega_{\text{baryon}}, t_{\text{shock}}), \quad (9)$$

where $M_{\text{shock}} = M_{\text{gas}}(r_{\text{shock}}) = \Omega_{\text{baryon}} M_{\text{DM}}(r_{\text{shock}})$. Figure 4 shows plots of r_{shock} vs. M_{shock} for the four halos shown in Figure 1 obtained from solving the above equation and compares it to that obtained using a spherically symmetric Lagrangian hydro-dynamics code similar to that of Thoul & Weinberg 1995. Both results obey a simple power law

$$\frac{r_{\text{shock}}}{r_{\text{halo}}} \approx \left(\frac{M_{\text{shock}}}{\Omega_{\text{baryon}} M_{\text{halo}}} \right)^{\beta_{\text{shock}}}, \quad \beta_{\text{shock}} \approx 0.82. \quad (10)$$

In the next two sections this result is used to estimate the gas properties of the bulge and the disk.

3.4. Initial Bulge

Inside the shock the gas is approximately isothermal with a temperature given by $T_{\text{shock}} = \alpha_T V_{\text{circ}}^2(r_{\text{shock}})$. In addition, the gas will be in hydrostatic equilibrium. In the case of a DM halo with a flat rotation curve, the density of the gas just inside the shock is

$$\rho_{\text{shock}} = \rho_{\text{gas}}(r_{\text{shock}}) \approx \frac{M_{\text{shock}}}{\frac{4\pi}{3-\alpha_T} r_{\text{shock}}^3}, \quad (11)$$

If the cooling time is short compared to the dynamical time, then clumps in the shocked gas will condense and form the first bulge stars, otherwise they will spiral inwards until they hit the disk. The boundary between gas that cools quickly and gas that hits the disk can be computed by setting $t_{\text{dyn}}(r_{\text{shock}}) = t_{\text{cool}}(r_{\text{shock}})$:

$$\frac{\pi r_{\text{shock}}}{2 V_{\text{circ}}} = \frac{\rho_{\text{shock}} k_B T_{\text{shock}}}{(\gamma - 1)\mu} \frac{\mu^2}{\Lambda(T_{\text{shock}}) \rho_{\text{shock}}^2}, \quad (12)$$

where $\Lambda(T)$ is the primordial optically thin cooling function (Thoul & Weinberg 1995), μ is the mean molecular weight, k_B is Boltzman's constant and $\gamma = \frac{5}{3}$. Manipulating the above expression gives

$$\frac{M_{\text{shock}}}{r_{\text{shock}}^2} = \frac{8}{3 - \alpha_T} \frac{\mu k_B T_{\text{shock}} V_{\text{circ}}}{(\gamma - 1) \Lambda(T_{\text{shock}})} \quad (13)$$

All the terms on the right can be obtained directly from the parameters specifying the DM halo. If M_{shock} and r_{shock} are related by a simple power law, then the initial mass and radius of the bulge can be estimated. Figure 5 shows $r_{\text{bulge}}^{\text{init}}$ and $M_{\text{bulge}}^{\text{init}}$ for four DM halos as a function of V_{circ} for $\alpha_T = 2$.

3.5. Disk Formation

Subsequent mass shells will split their material between the bulge and the disk depending upon the distribution of specific angular momentum within each mass shell. The simplest model for the initial angular momentum distribution is to assume that each shell is in solid body rotation with frequency ω_0 when $r = r_{\max}$, where $\omega_0 = \lambda_{\text{spin}} V_{\text{circ}} / r_{\text{halo}}$. This model is consistent with the idea that a typical proto-galaxy acquires the majority of its angular momentum from a single encounter with a similar sized object when it is at maximum expansion. In the bump initial conditions used here the inner shells will turn around before the outer shells. If the external torquing field changes in time, then the shells will have different angular momentum histories. This is most likely the case in the real galaxies. However, because solid body rotation does an adequate job of explaining the current state of disk galaxies (Dalcanton, Spergel & Summers 1997, Mo, Mao & White 1997), it is convenient to maintain this simplifying assumption.

The distribution of specific angular momentum within a rotating shell is not the same. Gas at the equator will have more angular momentum than gas at the poles. This distribution of specific angular momentum within a gas shell at a time when the shell is at a radius r_{gas} is $j_{\text{gas}} = (R_{\text{gas}}/r_{\text{gas}})^2 j_{\max}$, where $j_{\max} = \omega_0 r_{\max}^2$ and $R_{\text{gas}} \leq r_{\text{gas}}$ is the projected radius. The specific angular momentum of each radius in the DM halo is $j_{\text{DM}} = V_{\text{circ}}(R_{\text{DM}})R_{\text{DM}}$. The final distribution of the gas can be computed by setting $j_{\text{gas}} = j_{\text{DM}}$

$$M_{\text{gas}}(R_{\text{DM}}) = \left\{ 1 - \sqrt{1 - j_{\text{DM}}(R_{\text{DM}})/j_{\max}} \right\} M_{\text{gas}}^{\text{tot}}, \quad (14)$$

The majority of the mass of each shell ends up near the maximum radius $j_{\text{DM}}(R_{\text{DM}}) = j_{\max}$, which for an isothermal halo is $R_{\text{DM}} = j_{\max}/V_{\text{circ}}$. The final distribution of the disk can be computed by summing the contributions of each gas shell. Detailed calculations of this type reproduce a wide range of observed properties (Dalcanton, Spergel & Summers 1997, Mo, Mao & White 1997).

The gas takes approximately $t_{\text{dyn}}(r_{\text{shock}})$ to settle into the above distribution after it has been shocked. Because the majority of each gas shell falls near the maximum angular momentum radius, the disk grows outward according to $r_{\text{disk}}^{\max}(t_{\text{shock}}(M_{\text{shock}}) + t_{\text{dyn}}(M_{\text{shock}})) = j_{\max}(M_{\text{shock}})/V_{\text{circ}}$. This outer edge will grow as long as there is infalling material.

In contrast, the bulge continues to grow by slowly accumulating the low specific angular momentum material of many gas shells. The total amount of material falling into the bulge can be computed by integrating the shocked shells

$$M_{\text{bulge}}(t_{\text{shock}}(M_{\text{shock}}) + t_{\text{dyn}}(M_{\text{shock}})) = \int_0^{M_{\text{shock}}} \left\{ 1 - \sqrt{1 - j_{\text{DM}}(r_{\text{bulge}})/j_{\max}(M'_{\text{shock}})} \right\} dM'_{\text{shock}} \quad (15)$$

In general, $t_{\text{dyn}} + t_{\text{shock}} \approx t_{\text{collapse}}$, so for any halo:

$$M_{\text{bulge}}(t_{\text{collapse}}(M_{\text{shock}})) = \int_0^{M_{\text{shock}}} \left\{ 1 - \sqrt{1 - \frac{V_{\text{circ}}(r_{\text{bulge}})r_{\text{bulge}}r_{\text{halo}}}{V_{\text{circ}}(r_{\text{halo}})\lambda_{\text{spin}}r_{\max}(M'_{\text{shock}})}} \right\} dM'_{\text{shock}} \quad (16)$$

The gas in the disk is simply $M_{\text{disk}} = M_{\text{shock}} - M_{\text{bulge}}$. Figure 6 shows the evolution of the infall rates \dot{M}_{bulge} and \dot{M}_{disk} as a function of redshift for four different DM halos. Interestingly, this very simple picture produces old bulges and young disks quite naturally, with reasonable values for the total mass and infall rates.

3.6. Blowout

The bulge will continue to grow slowly without additional sources of energy to heat the gas and drive a wind. There are three potential sources of energy input: Supernovae Type I, Supernovae Type II and a massive black hole. A realistic treatment of the feedback due to any of these processes is a challenging undertaking and is fundamentally limited by an incomplete understanding of several processes (e.g., star formation, supernova IMF, black hole formation, etc ...). Here only the most simple estimates are attempted. Fundamentally, to drive a wind the energy input into the bulge gas must overcome the escape velocity of the infalling gas:

$$\dot{M}_{\text{bulge}} V_{\text{esc}}^2 < \max\{\alpha_{\text{SNI}} L_{\text{SNI}}, \alpha_{\text{SNII}} L_{\text{SNII}}, \alpha_{\text{BH}} L_{\text{BH}}\} \quad (17)$$

where V_{esc} is the typical escape velocity of gas in the bulge, and $\alpha_{\text{SNI},\text{SNII},\text{BH}}$ is the fraction of the total energy input of each type which is usefully deposited into the gas in such a way as to drive a wind, i.e. a parameterization of our ignorance about converting luminosities into winds. The energy inputs can be estimated as follows

$$L_{\text{SNI}} = \epsilon_{\text{SNI}} M_{\text{bulge}} V_{\text{SNI}}^2 / t_{\text{SNI}} \quad (18)$$

$$L_{\text{SNII}} = \epsilon_{\text{SNII}} \dot{M}_{\text{bulge}} V_{\text{SNII}}^2 \quad (19)$$

$$L_{\text{BH}} = \epsilon_{\text{BH}} \dot{M}_{\text{BH}} c^2 \approx L_{\text{edd}} = M_{\text{BH}} c^2 / t_{\text{edd}} \quad (20)$$

where, $t_{\text{edd}} = \frac{\sigma_T c}{4\pi G m_H} \approx 5 \times 10^9$ yr.

The equation for L_{SNI} assumes the progenitors of Type I SN (really Type Ia) are white dwarfs or some other compact stellar remnant which should be proportional to the total bulge population. If the average rate of SNI is one per hundred years per 10^{10} M_\odot (Pain et al 1996) and each SNI ejects approximately $1 M_\odot$ of material, then setting $\epsilon_{\text{SNI}} \sim 0.01$, $V_{\text{SNI}} \sim 10^4$ km s $^{-1}$ and $t_{\text{SNI}} \sim 10^{10}$ yr will give approximately the correct rates and energies for SNI.

The equation for L_{SNII} assumes the progenitors of Type II SN (really Type Ib,c and Type II) are massive short lived stars whose rate should be proportional to the star formation rate, which in turn is roughly proportional to the infall rate. If the average rate of SNII is once per hundred years (Cappellaro et al 1997) in galaxies with star formation rates and infall rates of on the order of one solar mass per year, and each SNII also ejects $\sim 1 M_\odot$ of material, then setting $\epsilon_{\text{SNII}} \sim 0.01$ and $V_{\text{SNI}} \sim 10^4$ km s $^{-1}$ will give approximately the correct rates and energies for SNII.

The equation for L_{BH} assumes the massive black hole radiates a fraction of the gravitational

energy of the material falling onto it. Furthermore, it assumes that the luminosity and subsequently the infall rate is constrained by the Eddington luminosity of the black hole.

Using these definitions it is possible to try and guess under what conditions each type of energy input will drive a wind. The blowout condition for Type II Supernova is the simplest

$$V_{\text{esc}} < V_{\text{SNII}} \alpha_{\text{SNII}}^{\frac{1}{2}} \epsilon_{\text{SNII}}^{\frac{1}{2}}, \quad (21)$$

The value of α_{SNII} is difficult to estimate, but can be obtained by setting $V_{\text{esc}} \sim 100 \text{ km s}^{-1}$ the equivalent critical value arrived at in more detailed calculations (Dekel & Silk 1986), in which case $\alpha_{\text{SNII}} \sim 0.01$.

For Type I Supernova the blowout condition is

$$\dot{M}_{\text{bulge}} V_{\text{esc}}^2 < \alpha_{\text{SNI}} \epsilon_{\text{SNI}} M_{\text{bulge}} V_{\text{SNI}}^2 / t_{\text{SNI}}, \quad (22)$$

which can be rewritten in terms of the bulge growth time $M_{\text{bulge}}/\dot{M}_{\text{bulge}}$

$$V_{\text{esc}} < V_{\text{SNI}} \left(\frac{\alpha_{\text{SNI}} \epsilon_{\text{SNI}} M_{\text{bulge}}}{t_{\text{SNI}} \dot{M}_{\text{bulge}}} \right)^{\frac{1}{2}}. \quad (23)$$

The above condition is plotted in Figure 7 (along with the SNII condition) assuming the $\alpha_{\text{SNI}} = \alpha_{\text{SNII}}$.

This oversimplified model does not readily produce a black hole blowout condition, but it is possible to estimate the ratio of the black hole mass to the bulge. If the black hole accretion is limited by the Eddington luminosity, then $M_{\text{BH}} = M_{\text{BH}}^{\text{init}} \exp[t/\epsilon_{\text{BH}} t_{\text{edd}}]$, which sets the time scale for blowout $t_{\text{blowout}} = \epsilon_{\text{BH}} t_{\text{edd}} \ln[M_{\text{BH}}/M_{\text{BH}}^{\text{init}}]$. Combining the equation for black hole luminosity with the blowout condition gives

$$M_{\text{BH}} > \frac{t_{\text{edd}} V_{\text{esc}}^2}{\alpha_{\text{BH}} c^2} \dot{M}_{\text{bulge}} \quad (24)$$

If accretion onto the bulge is relatively constant, then $\dot{M}_{\text{bulge}} \sim M_{\text{bulge}}/t_{\text{blowout}}$ and the ratio of the black hole to the bulge at blowout is

$$\left(\frac{M_{\text{BH}}}{M_{\text{bulge}}} \right)_{\text{blowout}} > \frac{(V_{\text{esc}}/c)^2}{\alpha_{\text{BH}} \epsilon_{\text{BH}} \ln[M_{\text{BH}}/M_{\text{BH}}^{\text{init}}]}, \quad (25)$$

which for the characteristic numbers $\epsilon_{\text{BH}} \ln[M_{\text{BH}}/M_{\text{BH}}^{\text{init}}] \sim 1$ and $V_{\text{esc}} \sim 100 \text{ km s}^{-1}$ requires a value of $\alpha_{\text{BH}} > 10^{-4}$ in order to be in agreement with the observed black hole to bulge ratio of $\sim 10^{-3}$ (Faber et al 1996). Using this bound for α_{BH} we can now estimate the blowout condition

$$V_{\text{esc}} < \left(\frac{c^2 \alpha_{\text{BH}}}{t_{\text{edd}}} \frac{M_{\text{bulge}}}{\dot{M}_{\text{bulge}}} \right)^{\frac{1}{2}} \left(\frac{M_{\text{BH}}}{M_{\text{bulge}}} \right)_{\text{blowout}}^{\frac{1}{2}}, \quad (26)$$

which is also shown in Figure 7 for $\alpha_{\text{BH}} = 10^{-3}$.

4. Discussion

The previous sections synthesized an inside-out galaxy formation scenario by combining a spherical collapse model with the final redistribution of gas by angular momentum. The aim was to interpolate the gaseous evolution from models of the initial and final states of the DM and the gas.

The DM is governed by the specified final halo profile and r_{\max} and t_{collapse} , which are set by the mass overdensity of the initial profile δ_m . The primary focus here is on the gas, and its response to the DM potential. Thus, a highly simplified model is adopted of the post-collapse state of each DM halo. Each DM shell stops falling at the radius given by a pre-set final DM profile. The validity of this approximation is questionable. Clearly it cannot properly account for any hierarchical buildup of material in the halo. If, however, DM halos—in spite of hierarchical accretion—maintain a quasi-self-similar density profile as is suggested from N-body simulations (Navarro, Frenk & White 1996), then this asymptotic approach might be OK.

The state of the gas can be characterized by the evolution of the adiabatic shock in response to the above DM potential. For Gaussian initial conditions, r_{shock} and M_{shock} can be related by simple power law (Figure 4) for a variety of DM halos. As mentioned earlier the adiabatic value of $r_{\text{shock}}(M_{\text{shock}})$ is only an upper limit. In a real multi-phase gas, r_{shock} will be smaller due to by the fraction of gas residing in cold clumps. This effect will be most pronounced earlier on, but during later stages of the infall the adiabatic approximation is in good agreement with similar calculations that take cooling into account (Thoul & Weinberg 1995).

Using the power law for the shock evolution, the size of the initial bulge (Figure 5) can be estimated by computing the cooling time just inside the shock and setting it equal to the dynamical time computed from the DM halo. It is reassuring that the initial bulge mass and radius are reasonable and display the correct dependence on the halo parameters, except for the Burkert profile, which is only meant for dwarf galaxy halos with $V_{\text{circ}} \leq 50 \text{ km s}^{-1}$. Unfortunately, the sensitivity of these estimates to α_T and to the details of the DM halo make this approach unsuitable for precise calculations.

After the infalling gas has been shocked, if it does not cool quickly and form stars, then it will spiral in to its corresponding angular momentum radius in about a dynamical time. The simplest model for the angular momentum of the gas is to assume that when each gas shell reaches its maximum radius it is in approximately solid body rotation with a frequency determined by λ_{spin} . What is most interesting is the relative ease with which one gets an old bulge and a young disk from this highly idealize picture. The infall rates (Figure 6), which are upper limits, are only a factor 10 greater than those seen observationally. The size of the disk vs. the bulge depends upon the quantity $r_{\text{bulge}}r_{\text{halo}}\lambda_{\text{spin}}$, thus there is a large amount of freedom to create diverse objects. More complex angular momentum models (Ryden & Gunn 1987, Eisenstein & Loeb 1995), which take into account the spectrum of initial fluctuations and estimate the statistical distribution of angular momentum, could also be used. The overall effect of these models would be to shift and

soften the transition between bulge and disk infall.

The bulge will continue to grow slowly and may be halted if there is sufficient energy input from supernova and/or a massive black hole to drive a wind. The disk will continue to grow outward as long as there is infalling material to supply it. The simple blowout estimates computed in the previous section indicate that all the mechanisms examined have the potential to drive a wind which may affect the accretion onto the bulge.

5. Conclusions and Further Work

A simple inside-out scenario for galaxy formation is presented, which is a natural result of synthesizing earlier work on DM halos, spherical collapse, and redistribution via angular momentum. The scenario predicts a straightforward sequence of events beginning with the formation of an initial bulge due to the high densities and rapid cooling times that exist when the first infalling mass shells are shock heated. After the initial collapse, the bulge continues to grow slowly but may be halted by energy input from supernova and/or a massive black hole initiates a wind that blows out the gas. A disk forms as the outermost shells collapse. The higher virial temperatures and lower gas densities of these shells result in longer cooling times; so that instead of quickly forming stars the gas spirals in towards its corresponding angular momentum radius.

Although, this model is highly simplified and is not designed to accurately describe the formation of any individual galaxy, it does (by design) predict the overall features of galaxies. In addition, it appears that old bulges and young disks are an almost unavoidable result of this very simple model. Furthermore the epochs at which maximum infall into the bulge and inner disk take place are roughly consistent with both the high star formation rates (Madau, Pozzetti & Dickinson 1997) and quasar densities (Boyle et al 1997) observed at $z \sim 2$. A blowout taking place early in the evolution of a galaxy is also consistent with the observation of high velocity winds seen at high redshift (Pettini et al 1997). This scenario also suggests two mechanisms for preventing the formation of disk galaxies in the center parts of clusters. First, by encounters which disrupt the alignment of the angular momentum vectors of the infalling gas. Second, by the high virial temperatures present, which would cause late infall to be absorbed into the ambient cluster gas. Of course, these are only two of many possible explanations, but never-the-less they may be worth exploring with more detailed simulations.

These simple calculations suggest an idealized framework in which to attempt the direct simulation of disks. Cosmologically based simulations are limited by the need to construct the potential from particles, which leads to a significant increase in the complexity and duration of the computations. Observing 3D gas collapse into a spherically symmetric time evolving potential like the one presented here should be a useful test case of the 3D codes. Further work in this area should also focus on exploring the role of the processes that intrinsically cannot be included in this simple model: hierarchical structure formation and a multi-phase ISM.

Finally, the extremely simple estimates of the blowout condition suggest that Type I and Type II Supernovae and super massive black holes all have the potential to initiate an outflow and subsequently change the evolution of the bulge. Further calculations along these line using more realistic assumptions could prove fruitful in explaining the observed properties of bulges and elliptical galaxies.

I would particularly like to thank my advisor Professor Spergel for his important contributions to this work and many interesting and enjoyable conversations. I would also like to thank Professors Gunn, Ostriker, Strauss and Gott for their helpful comments. In addition, the comments of an anonymous referee much improved this paper. The author was supported by NSF grant AST 93-15368.

REFERENCES

- Bardeen, J., Bond, J., Kaiser, N. & Szalay, A. 1986, ApJ, 304, 15
- Bertschinger, E. 1985, ApJS, 58, 39
- Borgani, S., Moscardini, L., Plionis, M., Gorski, K.M., Holtzman, J., Klypin, A., Primack, J.R., Smith, C.C. & Stompor, R. 1997, New Astronomy, 1 ,321
- Burkert, A. 1995, ApJ, 447, L25
- Boyle, B., Smith, R., Shanks, T., Croom, S. & Miller, L., 1997, astro-ph/9710202
- Cappellaro, E., Turatto, M., Tsvetkov, D. Yu., Bartunov, O. S., Pollas, C., Evans, R. & Hamuy, M. 1991, A&A, 322, 431
- Dalcanton, J., Spergel, D., & Summers, F. 1997, ApJ, 482, 659
- Dekel, A. & Silk, J. 1986, ApJ303, 39
- Eisenstein, D., & Loeb, A. 1995 ApJ, 439, 520
- Faber, S.M., Tremaine, S., Ajhar, E., Byun, Y., Dressler, A., Gebhardt, K., Grillmair, C., Kormendy, J., Lauer, T. & Richstone, D. 1996, astro-ph/9610055
- Fall, S. & Efstathiou, G. 1980, MNRAS, 193, 189
- Fillmore, J., & Goldreich, P. 1984, ApJ, 281, 1
- Gunn, J., & Gott, R. 1972, ApJ, 176, 1
- Gunn, J. 1982, in *Astrophysical Cosmology*, ed. H.A. Bruck, G.V. Coyne & M.S. Longair, (Vatican: Pontifica Acadamia Scientiarum), 191

- Hernquist, L. 1990, ApJ, 356, 359
- Hoffman, Y. 1988, ApJ, 328, 489
- Katz, N., Weinberg, D.H., & Hernquist, L. 1996, ApJS, 105, 19
- Kepner, J., Babul, A. & Spergel, D. 1997, ApJ, 487, 61
- Lacey, C. & Cole., S. 1994, MNRAS, 271, 676
- Ma, C., Bertschinger, E., Hernquist, L., Weinberg, D. & Katz, N. 1997, ApJ, 484, L1
- Madau, P., Pozzetti, L. & Dickinson, M. 1997, astro-ph/9708220
- Mestel, L. 1993, MNRAS, 126, 553
- Miralda-Escude, J., Cen, R., Ostriker, J. & Rauch, M. 1996, ApJ, 471, 582
- Mo, H., Mao, S., & White, S. 1997, astro-ph/9707093, ApJ, submitted
- Navarro, J.F., Frenk, C.S., & White, S.D.M. 1996, astro-ph/9611107, ApJ, submitted
- Navarro, J.F., & Steinmetz, M. 1997, ApJ, 478, 13
- Pain et al 1996, ApJ, 473, 356
- Pettini, M., Steidel, C., Dickinson, M., Kellogg, M., Giavalisco, M. & Adelberger, K., 1997, astro-ph/9707200
- Ryden, B., & Gunn, J. 1985, AJ, 318, 15
- Steinmetz, M. & Ewald, M. 1995, MNRAS, 276, 549
- Thoul, A., & Weinberg, D.H. 1995, ApJ, 442, 480
- Thoul, A., & Weinberg, D.H. 1996, ApJ, 465, 608
- Zhang, Y., Meiksin, A., Anninos, P. & Norman, M. 1997, ApJ, in press

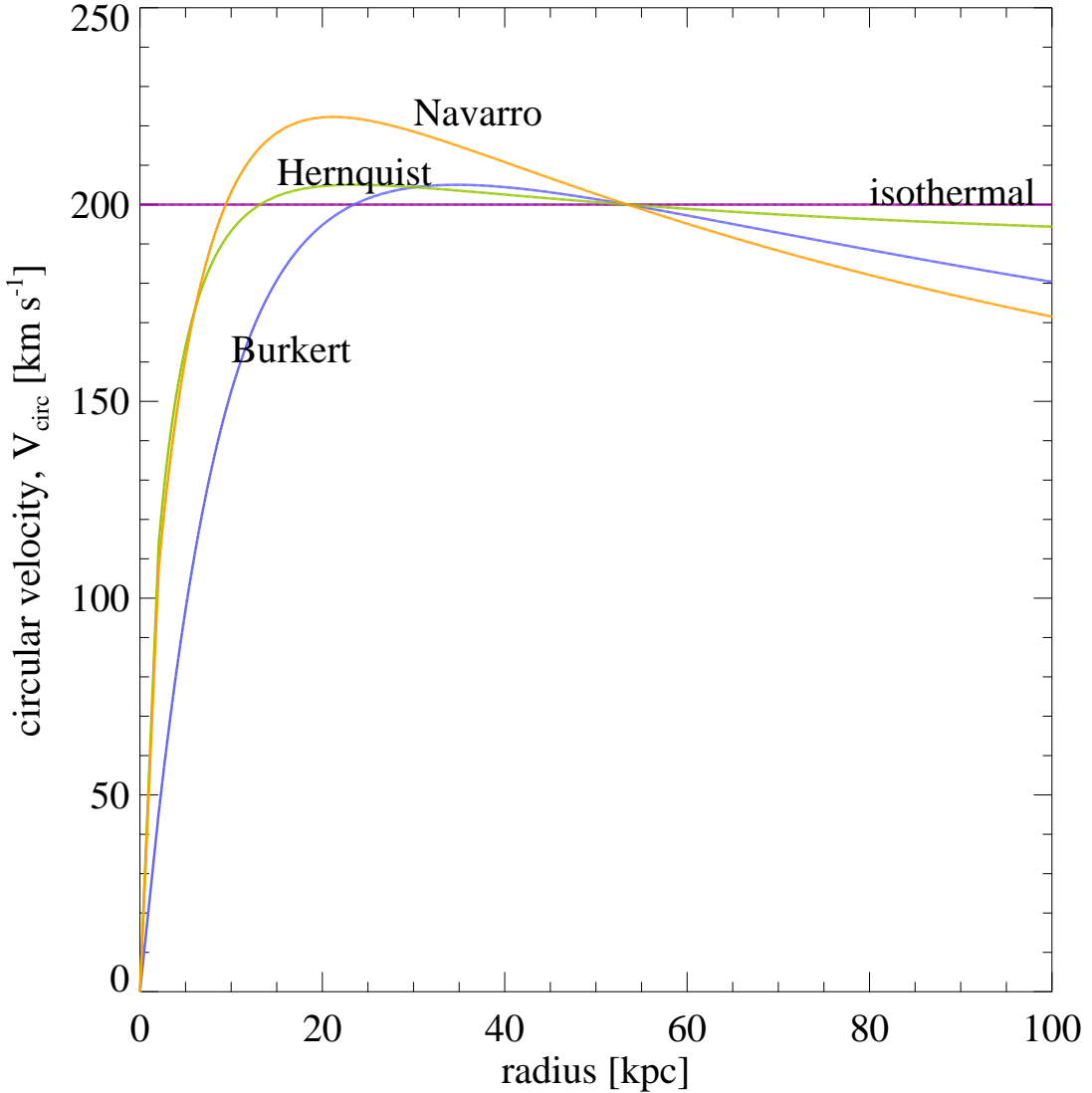


Fig. 1.— The circular velocities for different profiles for a DM halo with $V_{\text{circ}}(r_{\text{halo}}) = 200 \text{ km s}^{-1}$, $z_{\text{virial}} = 3$, $M_{\text{halo}} = 10^{12} M_{\odot}$, $r_{\text{halo}} = 54 \text{ kpc}$. All the profiles reproduce typical rotation curves over the observable range. Hernquist: $M \propto r^2/(r + a)^2$, isothermal: $M \propto r$, Navarro: $M \propto \log(r^2 + a^2)$, Burkert: $\rho \propto [(r + a)(r^2 + a^2)]^{-1}$, where $5a = r_{\text{halo}}$.

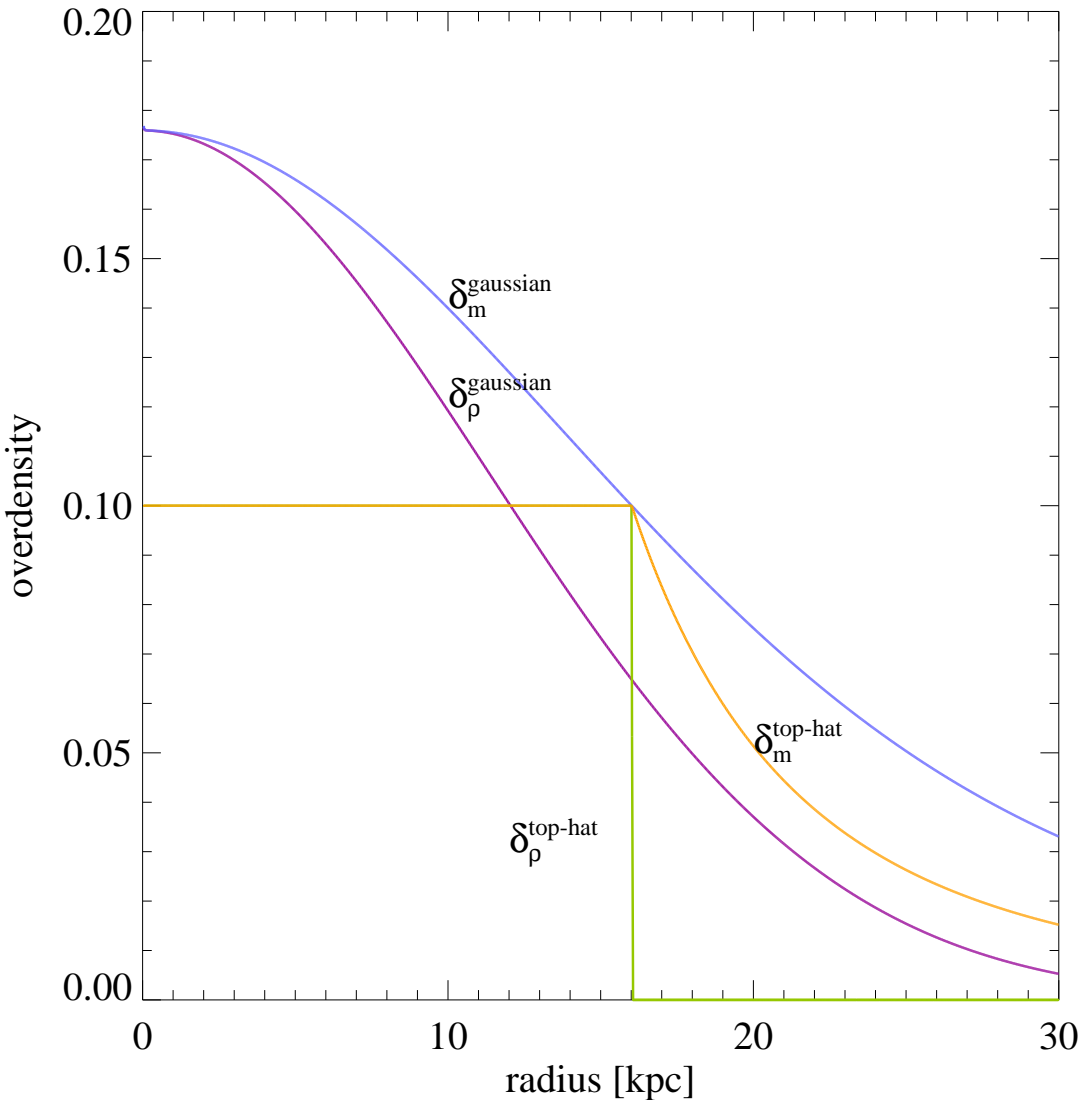


Fig. 2.— Initial density profile and initial mass overdensity profile obtained from a Gaussian bump, and a corresponding top-hat profile for the halo given in Figure 1 ($z_{\text{init}} = 68$, $r_{\text{halo}}(z_{\text{init}}) = 16$ kpc).

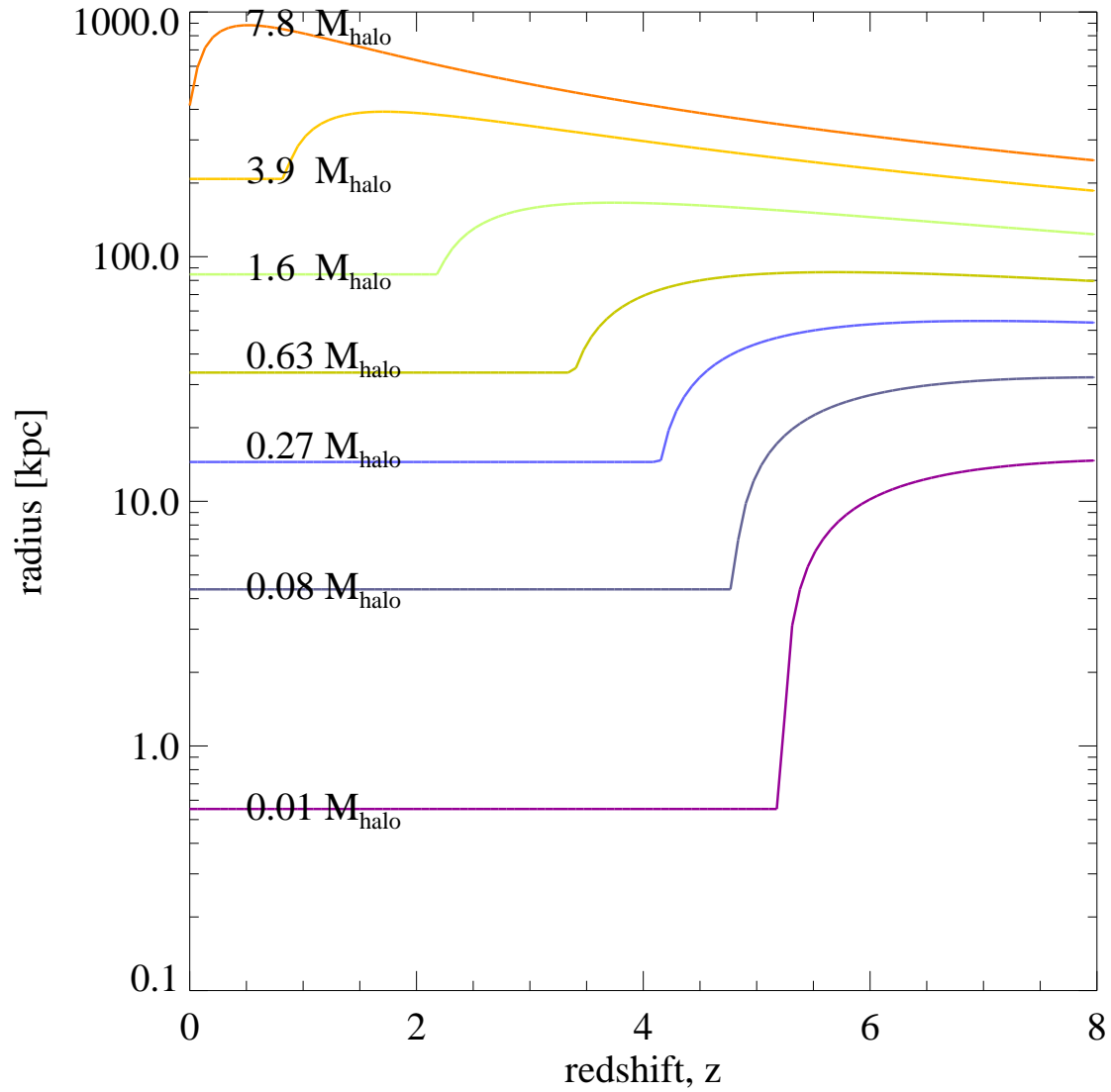


Fig. 3.— Trajectories of selected DM shells. The shells are stopped at the radius corresponding to the final position for the isothermal halo given in Figure 1.

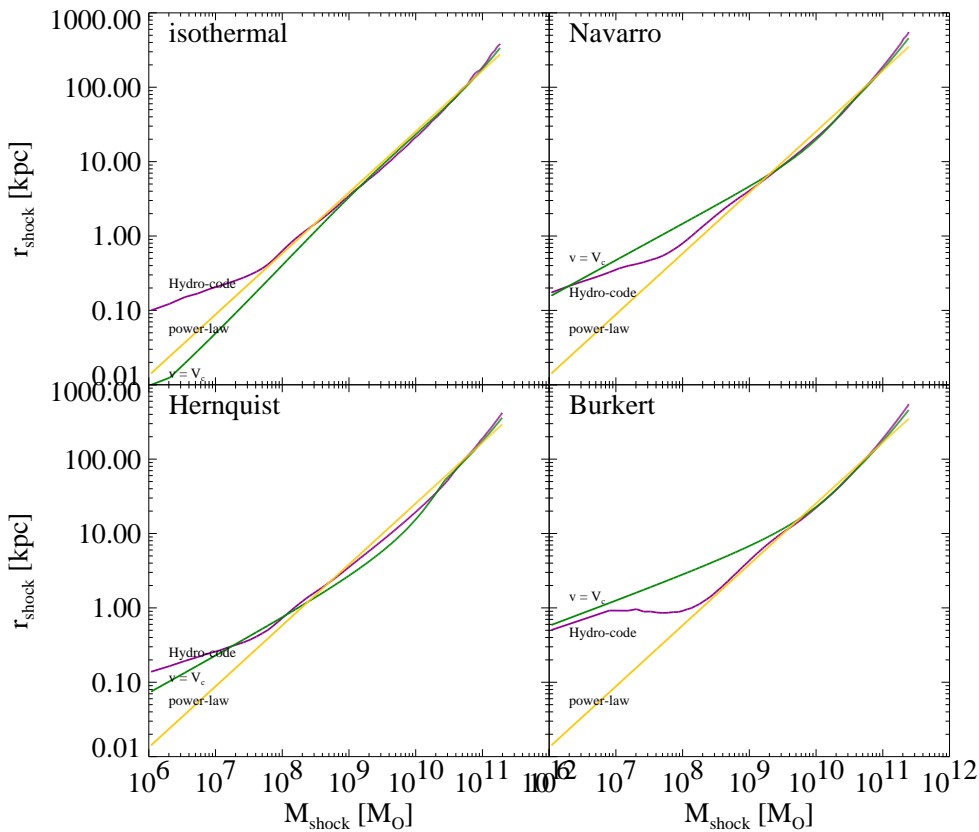


Fig. 4.— Shock radius r_{shock} vs shock mass M_{shock} for the four DM halos given in Figure 1 using three methods: (i) Lagrangian hydrodynamics code (ii) infall velocity constraint $V_{\text{circ}}(r_{\text{shock}}) = v_{\text{DM}}(M_{\text{shock}})$ (iii) simple power law ($r_{\text{shock}}/r_{\text{halo}}$) = $(M_{\text{shock}}/\Omega_{\text{baryon}} M_{\text{halo}})^{\beta_{\text{shock}}}$, $\beta_{\text{shock}} = 0.82$.

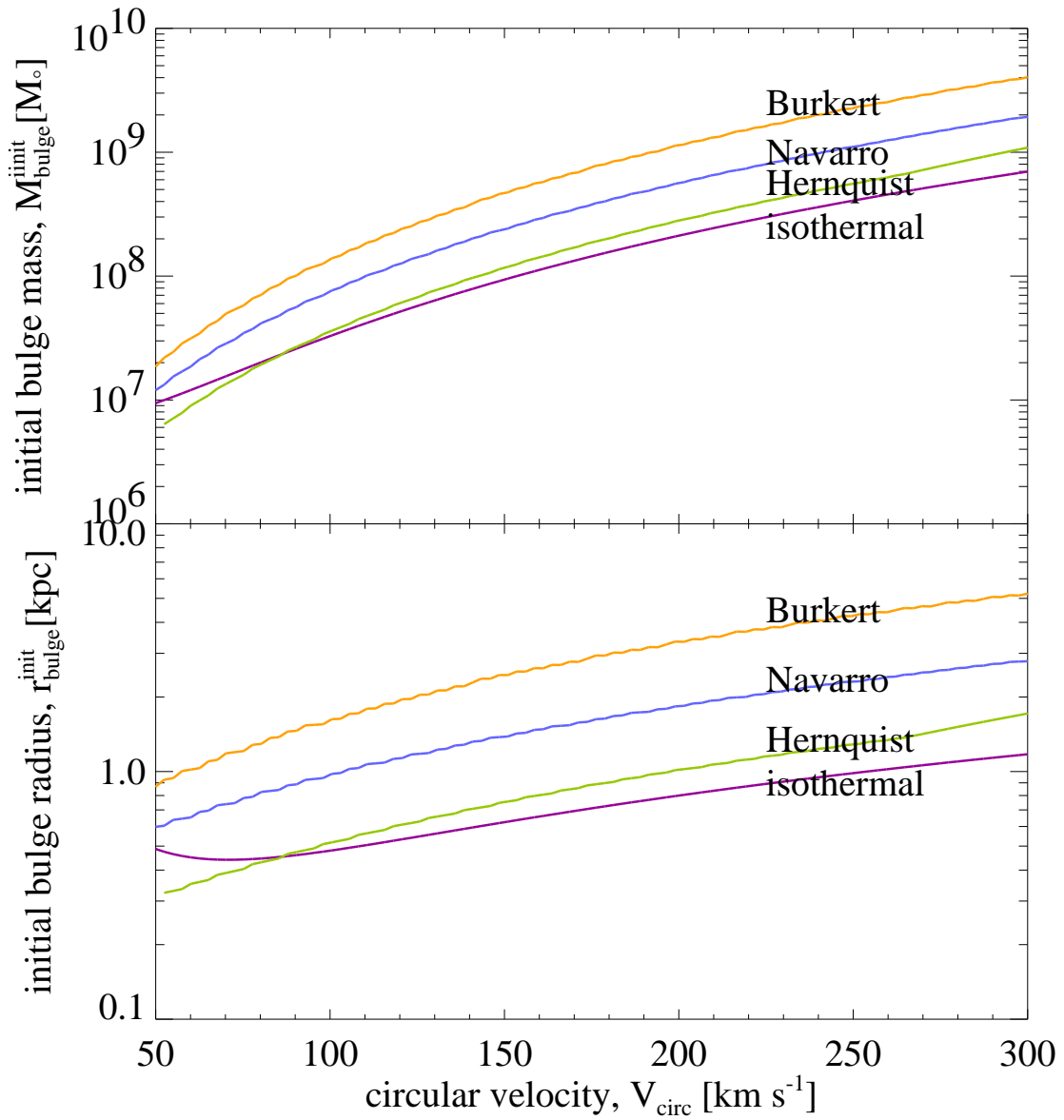


Fig. 5.— Initial bulge radius r_{bulge} and initial bulge mass M_{bulge} as a function of circular velocity computed for the four halos shown in Figure 1 assuming $z_{\text{virial}} = 3$.

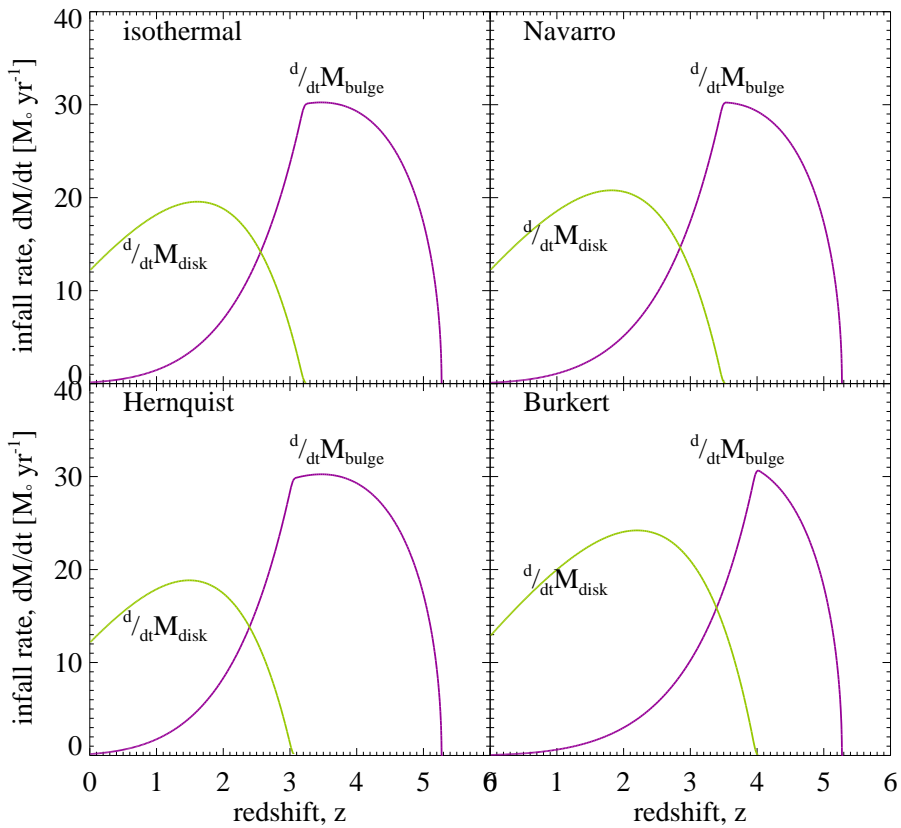


Fig. 6.— Disk and bulge infall rates vs. redshift for four DM halos with $V_{\text{circ}} = 200 \text{ km s}^{-1}$ and $z_{\text{virial}} = 3$ and $r_{\text{bulge}} = 4 \text{ kpc}$, $\lambda_{\text{spin}} = 0.03$.

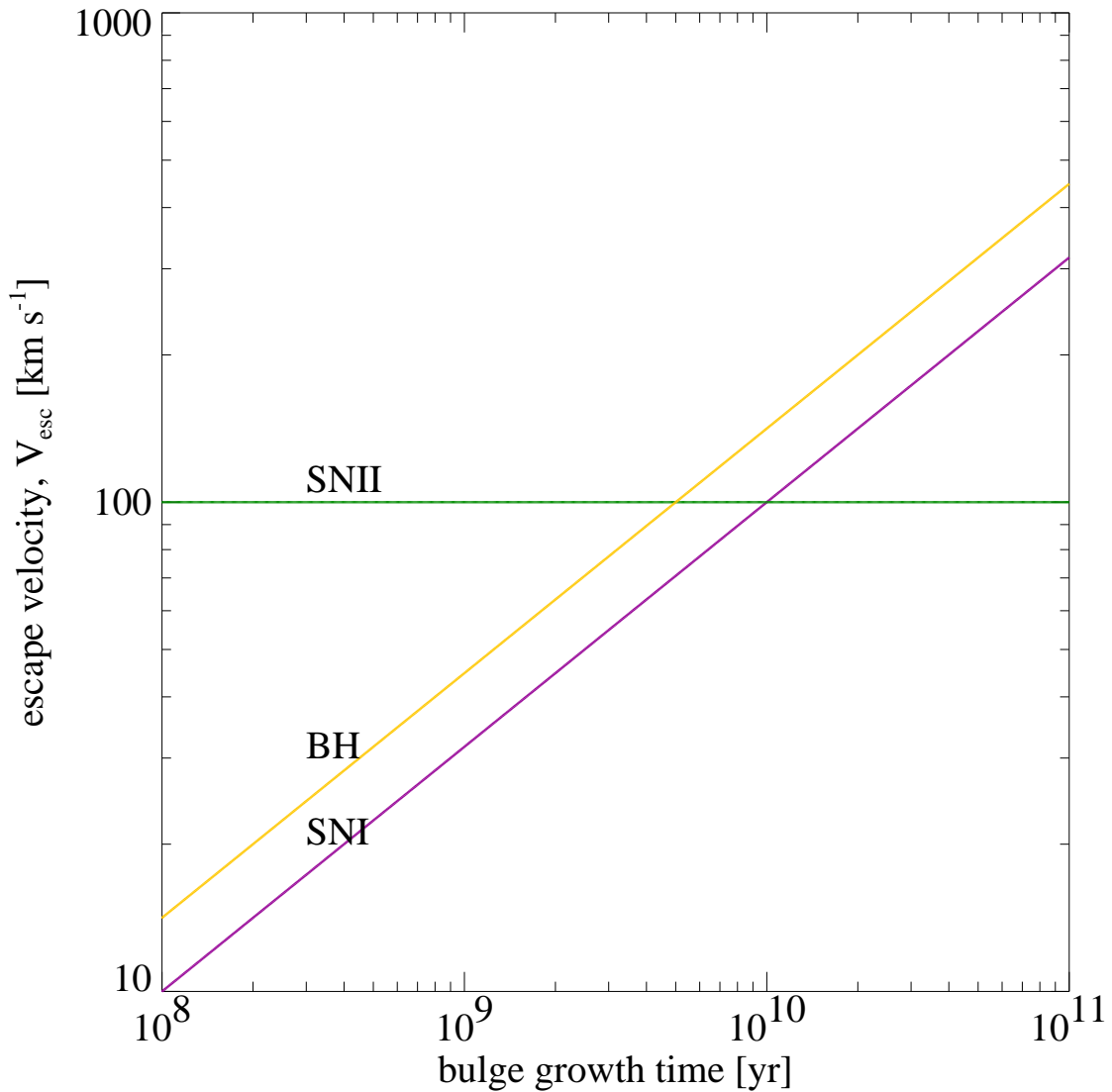


Fig. 7.— Bulge blowout conditions for Type I and Type II supernova and a super-massive black hole.